Combined positive-sequence flux estimation and current balancing for sensorless motor control under imbalanced conditions

Georgios I. Orfanoudakis *Member, IEEE,* Suleiman M. Sharkh, *Senior Member, IEEE,* and Michael A. Yuratich

***Abstract*— Sensorless motor control under imbalanced conditions, commonly caused by the use of an imbalanced cable, poses a number of challenges relating to stability and power quality. With reference to stability, concerns arise because the angle and frequency estimates of conventional PLLs and observers deteriorate in the presence of imbalance, which in turn degrades the response of synchronous-reference-frame current controllers. Power quality is also degraded due to the asymmetry of the currents supplied to the motor, which results in torque ripple and increased motor losses. In this paper, an adaptive positive-sequence flux estimator based on Second-Order Generalized Integrators (SOGI) is presented to solve these problems. The balanced fluxes generated by the estimator are suitable for PLL-based sensorless control of a motor over an imbalanced cable. With negligible additional computational effort, the flux estimator also provides negative-sequence current estimates, which are then controlled to balance the motor currents. Simulation and experimental results with a permanent magnet synchronous motor (PMSM) run by a commercial motor drive via a flat long Electrical Submersible Pumping (ESP) cable are presented. It is shown that the proposed method can prevent instabilities that occur when using conventional flux estimation methods and reduce current imbalance by approximately 10 to 20 times, to less than 1%.**

***Index Terms*— Asymmetry, Electrical Submersible Pumping (ESP), Flux estimator, Imbalance, Phase-Locked Loop (PLL), Second-Order Generalized Integrator (SOGI), Sensorless vector control, Unbalance**

I. Introduction

Power electronic motor drives, also referred to as Variable Frequency Drives (VFDs) are increasingly employed for the control of electric motors. In a variety of applications, such as electrical submersible pumps (ESPs), subsea booster pumps, downhole electric drilling, remotely operated vehicles and nuclear power plants or similar challenging environments, the motor is connected to the drive via a long cable [1 – 9]. The cable commonly has three cores, for power transmission only, and no signal wires. A sine filter followed by step-up transformer are commonly placed after the drive to reduce d*v*/d*t* and associated cable reflections and compensate for the cable voltage drop, respectively. With reference to control strategies, scalar (V/f - type) methods applied in the past are gradually substituted by vector control approaches, for which sensorless operation is mandatory due to the difficulty of transmitting the position information over long distances [2], [3], [5], [6], [8], [9], [10], [11].

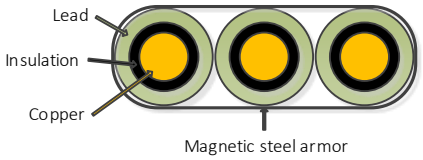

Fig. 1. Typical cross-section of flat steel-armored cable for ESP motors.

The basis for stable and efficient sensorless vector control lies on accurate motor flux estimation. Flux-based rotor position estimation is preferred to back-EMF based methods, due to the independence of the motor flux from the motor speed. Nevertheless, the integration required to obtain the flux poses its own challenges, as traditional integrators suffer from the known problems of drift/saturation due to DC offsets. To suppress those, integrators are typically combined with high-pass filters (HPF), which slow the integrator dynamics and can affect system stability. In motor control applications, these filters often need to be adaptive, to allow operation in an extended frequency range.

Motor flux estimation can also be affected by imbalances in the driven electrical system. For most applications, imbalance is commonly not a concern, as the driven motors are generally well balanced. In the presence of a long cable, however, the driven system (cable and motor) may not be balanced. Certain cables, especially flat steel-armored types with a typical cross-section as shown in Fig. 1, have substantially imbalanced self and mutual inductances [12]. Even round cables exhibit imbalance, particularly when they are in proximity to steel tubing for their entire length [1]. The unequal cable impedances on the three phases result in imbalanced load currents and thus imbalanced estimated motor fluxes.

Conventional Synchronous Reference Frame (SRF) and other three-phase Phase-Locked Loops (PLLs) [13], [14], [15] used as flux observers in motor drives are heavily affected by imbalances in their input signals. Thus, cable imbalance results in a degradation of the angle-frequency

Manuscript received December 9, 2020. This work was supported by TSL Technology Ltd, Ropley, UK.

G. I. Orfanoudakis is with the Electrical and Computer Engineering department at the Hellenic Mediterranean University (HMU), Heraklion, Crete, Greece, 71410 (e-mail: gorfas@hmu.gr).

S. M. Sharkh is with the Faculty of Engineering and the Physical Sciences at the University of Southampton, SO17 1BJ, UK (e-mail: S.M.Sharkh@soton.ac.uk).

M. A. Yuratich is with TSL Technology Ltd, Ropley, SO24 0BG, UK (e-mail: mike.yuratich@tsltechnology.com).

estimates required for sensorless control. Furthermore, excessive imbalance can affect the current control loops of vector-controlled drives, due to the fact that currents are generated based on inaccurate angle estimates, thus they get distorted and in turn affect the following angle estimates. Under certain conditions, the angle and current distortion can gradually grow and lead to instability and loss of control. A representative experimental result illustrating this effect is included in Section VI of the present study.

Additional concerns arise due to the current imbalance itself, as it causes excess losses in the motor and cable, which can lead to premature failures [2]. The imbalance also results in a reduction of average motor torque and increase of torque ripple, which causes vibration and audible noise [1], [16], [17], [18], and lowers the drive power factor [19]. Current imbalance is present even in the case that the adopted observer is immune to flux imbalances (thus ensuring stable motor control), as conventional vector control is designed to act on balanced currents and generate a balanced set of three-phase voltages. For imbalanced loads, however, the drive output voltages need to be appropriately imbalanced in order to balance the currents. This is normally achieved by the addition of a negative-sequence current controller, as shown in [14]. Note that an observer immune to imbalance is still required, as the estimated fluxes will become imbalanced in this case due to the imbalance of the generated voltages.

The Second-Order Generalized Integrator (SOGI) [20] has been used in the literature to address issues related to filtering, integration and imbalance in motor drives and grid-connected converters [20 – 33]. However, these three issues have been addressed separately, thus not covering the cases of applications which require flux estimation and current control under imbalanced conditions.

This paper contributes in two ways to bridge this knowledge gap, with the aim of improving the sensorless control of three-phase motors driven over imbalanced cables. First, it proposes a modified SOGI-based structure for estimating the positive-sequence component of the motor fluxes, which is essential for stable vector control. Second, it extends the proposed structure to actively suppress current imbalance, thus preventing additional losses and associated problems in the motor and cable [34], [35].

The paper is structured as follows. Section II provides the required theoretical background. Section III contains a description of the proposed structure and explains how it can be applied for the control of a permanent magnet synchronous motor (PMSM). Section IV presents a controller structure extension to achieve current balancing. Finally, Sections V and VI include simulation and experimental results, illustrating the advantages offered by the proposed approach.

II. Theoretical Background

The structure of a SOGI can be seen in Fig. 2a, together with its use for the generation of a set of Direct and Quadrature signals with respect to the input v, named $v´$ and $qv´$, respectively. The whole structure is referred to as SOGI-QSG (QSG: Quadrature Signal Generator). It has been shown that [20]:

- The Direct output, $v´$, introduces no phase shift and acts as a band-pass filter on v around frequency $\omega´$.
- The Quadrature output, $qv´$, introduces a 90-degree phase shift and acts as a low-pass filter (LPF) on v above frequency $\omega´$. Note that the Quadrature output is not the integral of the input.

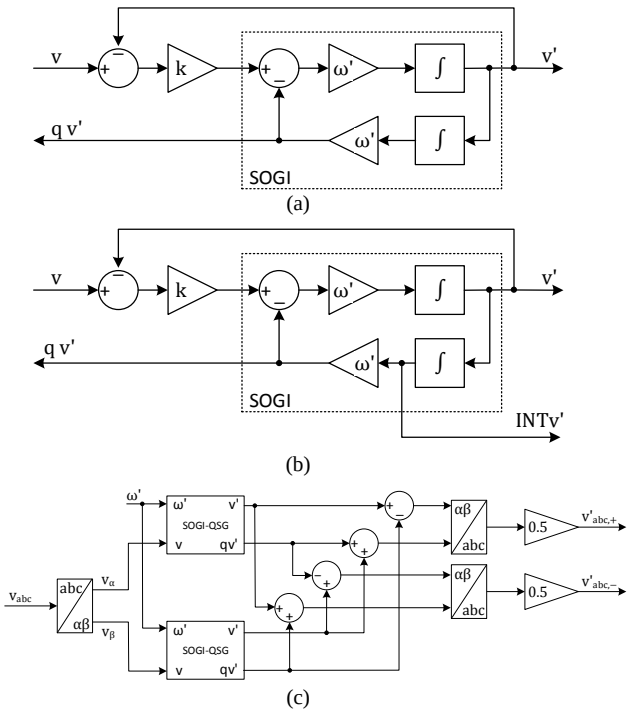

Fig. 2. (a) SOGI and SOGI-QSG [20], (b) SOGI-QSG with integrating output [24], (c) DSOGI with positive- and negative-sequence outputs [23].

The band-pass filtering characteristics of the Direct output can be used to suppress the distorting components of a sinusoidal signal with angular frequency $\omega´$. What is important is that $\omega´$ can vary, and can be supplied to the SOGI from a classic PLL, such as an SRF PLL. In this way, a SOGI-QSG and a PLL can act cooperatively: The SOGI-QSG cleans the input signals from distorting low- and high-frequency components, while the PLL works on cleaner signals, thus providing more stable and accurate frequency estimation to the SOGI-QSG, and to the user. Alternatively, $\omega´$ can be estimated by a Frequency-Locked Loop (FLL), as shown in [32], [33].

Apart from its use as an adaptive band-pass filter, the SOGI-QSG has been applied in the literature for the estimation of the filtered integral of the input signal, and more specifically for the estimation of flux from voltage, as shown in Fig. 2b [24], [29], [30], [31]. If v is a voltage, then $INTv´$ is the respective flux, filtered around frequency $\omega´$.

Furthermore, the Quadrature output of two SOGI-QSGs operating in the alpha-beta coordinates can be used as illustrated in Fig. 2c to form a Dual SOGI (DSOGI) structure [23] to extract the filtered positive-sequence component of the input signals, $v´_{abc,+}$, in an unbalanced 3-phase system. The extraction of the positive-sequence component is equivalent to the removal of imbalance. Moreover, the DSOGI structure can provide the negative-sequence component of the input signal, which relates to the imbalance between the three input signals. If the input signals are currents, then a set of synchronous reference frame current controllers can be used to suppress their imbalance, as explained in [14].

III. Flux Estimation Under Imbalanced Conditions

Techniques for removal of imbalance based on SOGI-QSGs have been applied in the literature only on the filtered output signals themselves. That is, the formation of a DSOGI has only been based on the non-integrating outputs, v' and qv'. In order to apply these techniques to the filtered integrals of the inputs, the Quadrature output for the integrating output, $INTv'$, must first become available. This section presents a method for extracting this output from a SOGI-QSG and subsequently creating a DSOGI structure which can provide the positive-sequence component of the integrals of a three-phase input. In the common case that the input is a set of three-phase voltages, the proposed structure provides a set of balanced fluxes [34], [35].

A. Proposed SOGI-2QSG and DSOGI_INT Structures

The sequence of the top multiplier and integrator in a SOGI-QSG can be altered (i.e. the integrator can be moved before the multiplier) without any effect on its transfer function. This minor modification offers the possibility of obtaining the Quadrature signal of $INTv'$, named $qINTv'$, as shown in Fig. 3. The transfer function for $qINTv'$ is the following:

$$H_{qINTv'} = qINTv'/v = -ks/(s^2 + k\omega' s + \omega'^2) \quad (1)$$

From the Bode diagram of this transfer function, plotted in Fig. 4 for $k = 1$ and $\omega' = 100$rad/s, it can be seen that if v is a voltage, then $qINTv'$ will be its Quadrature flux (amplitude = −40dB, phase = 180º), band-pass filtered around frequency ω'.

The overall structure resulting from the addition of the $qINTv'$ output, presented in Fig. 3, will be referred to as SOGI-2QSG, as it offers two QSGs in a single structure: a) The non-integrating QSG with outputs v' and qv', and b) the integrating QSG with outputs $INTv'$ and $qINTv'$. This provides a significant advantage with respect to the implementation of systems using this structure, as the same code or logic block can be used to generate all four signals.

The integrating outputs of a SOGI-2QSG can then be used in a DSOGI configuration (as in Fig. 2c), to obtain the positive sequence of the fluxes, $\psi_{abc,+}$, as shown in Fig. 5. Note that, if needed, the negative-sequence fluxes can also be generated by the same structure. This DSOGI configuration will be referred to as DSOGI_INT, to indicate that it generates (filtered and balanced) integrals of the input signals.

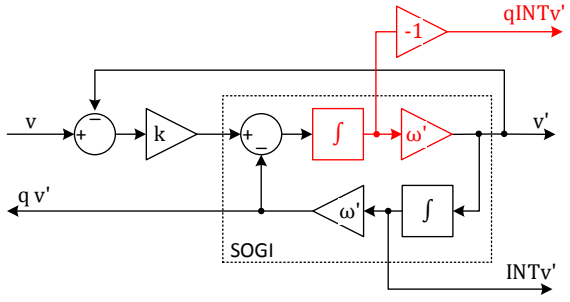

Fig. 3. Proposed structure SOGI-2QSG including a Quadrature integrating output.

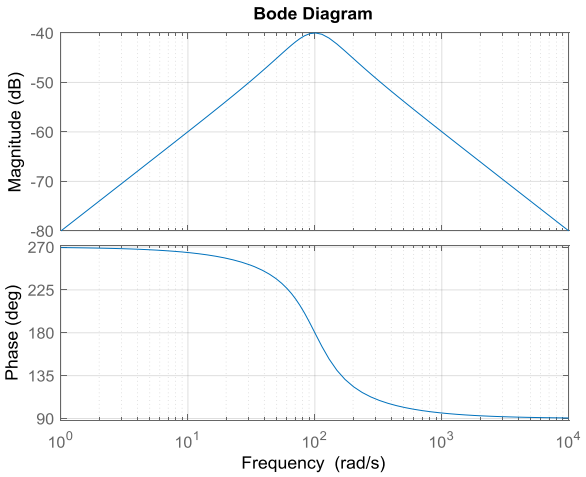

Fig. 4. Bode plot of the Quadrature flux output, qINTv′ (for k = 1, ω′ = 100rad/s).

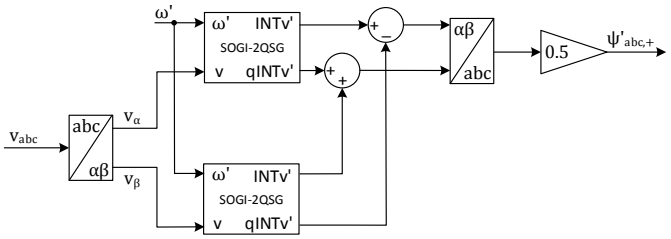

Fig. 5. DSOGI_INT using SOGI-2QSG's for the extraction of the positive-sequence fluxes ($\psi_{abc,+}$).

B. Application to Permanent Magnet Motor Control

For motor drive applications using imbalanced cables, the aim is to estimate the three (balanced) rotor fluxes. Using the case of a non-salient PMSM ($L_d = L_q = L$) as an example, the rotor fluxes, $\psi_{r,abc}$, are given by:

$$\psi_{r,abc} = \int (v_{abc} - Ri_{abc})dt - Li_{abc} \quad (2)$$

Assuming that the motor is driven by a VFD over a long cable, v_{abc} and i_{abc} are the generated phase output voltages and currents, while R and L are the total (i.e. cable and motor) phase resistance and inductance, respectively. Cable inductance is the parameter that can be unequal among the three phases, thus introducing imbalance in the system.

The parts of the equation for the flux that require integration should be passed to a DSOGI_INT (Fig. 5), whereas those that only need filtering should be passed to a DSOGI (Fig. 2c). In this case, the three-phase $(v - Ri)$ components need to be integrated and filtered, whereas the Li components only require filtering. Thus, a DSOGI_INT should be used for the $(v - Ri)$ components, while a DSOGI structure should be used for the Li components, as shown in Fig. 6. The respective abc outputs should then be subtracted and passed to a conventional PLL as explained in Section II, which will provide ω' for the DSOGI's. A Low-Pass Filter (LPF) may have to be applied on the estimated PLL frequency to produce ω'. The filter's time constant is typically in the range of 20ms, which is much lower than mechanical time constants relating to motor speed. An FLL can be used alternatively, as explained in [32], [33].

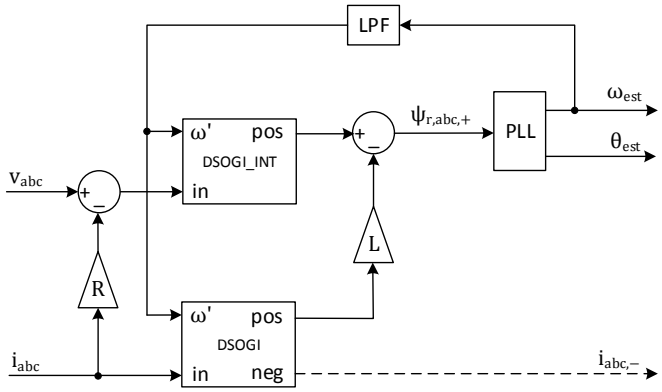

Fig. 6. Overall structure for PMSM rotor flux and frequency/angle estimation.

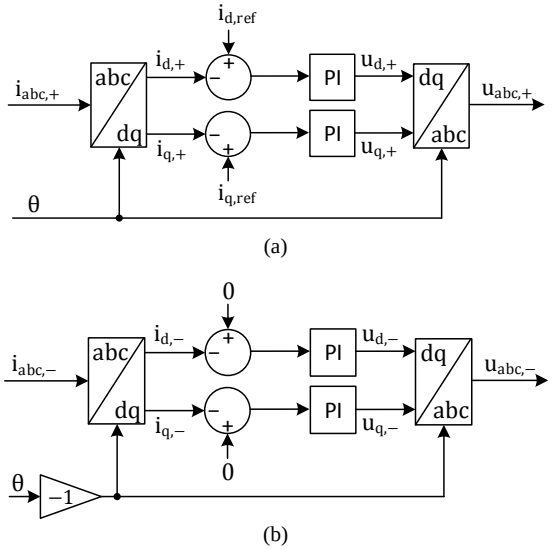

Fig. 7. (a) Positive- and (b) negative-sequence current controllers.

IV. Current Balancing

Although the above method can suppress the effect of imbalance on rotor flux angle estimation, the motor currents will still be imbalanced (as explained in Section I). In order to suppress the current imbalance, the conventional vector control approach shown in Fig. 7a can be extended with a set of PI controllers acting on the negative-sequence current in DQ coordinates and having zero reference values, as shown in Fig. 7b. The inputs to the positive- and negative-sequence controllers are the respective sets of currents ($i_{abc,+}$, $i_{abc,-}$), while their outputs are the inverter reference voltages ($u_{abc,+}$, $u_{abc,-}$). The derivation of the negative-sequence component can be performed by a DSOGI operating on the drive output currents. The synchronization method of Fig. 6 already includes such a DSOGI, which is favorable since the negative-sequence currents can be calculated with minimal additional computational cost (as compared to calculating the positive-sequence components only) by the same software block. Thus, according to the proposed approach, the implementation of the synchronization method is combined with the current control method as illustrated in Fig. 8, avoiding duplicate negative-sequence current calculation. The same principles can be applied for synchronization and current balancing in vector-controlled induction motors.

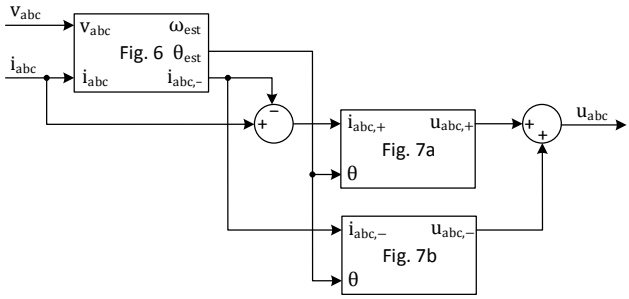

Fig. 8. Proposed combined PLL and current balancing approach.

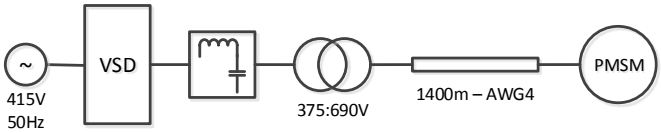

Fig. 9. Block diagram of the test setup.

V. Simulation Results

This section presents simulation results in MATLAB-Simulink, illustrating the outcomes from the application of the proposed method. The simulation model matches the experimental setup, which has the form of Fig. 9 and is described in detail in Section VI. The plots in Fig. 10 include drive output voltages and currents, estimated positive-sequence fluxes ($\psi_{r,abc,+}$ in Fig. 6), calculated positive- and negative-sequence currents, and percent imbalance according to the NEMA definition [36]. Two magnified extracts of the first column are also included to provide a clearer view on the effect of current balancing.

The results refer to the motor running at steady state with rated speed and torque. At the beginning of the plots (t = 5s), the positive-sequence flux estimator is in operation, while current balancing is disabled. The drive currents can be seen to be heavily imbalanced, which is also denoted by the high amplitude of the negative-sequence currents. The drive

TABLE I
Transformer and Cable Parameters

Transformer parameter	Value	Cable parameter	Value
Pri./Sec. voltage	375/690 V	Type	Flat, armored
Rated power	100 kVA	Size	AWG 4
Rated freq.	120 Hz	Length	1400 m
Impedance (pu)	4%	Resist. at 25C	1.17 Ω

TABLE II
Motor Parameters

Parameter	Value	Parameter	Value
Rated voltage	403 V	Pole pairs	2
Rated current	63 A	Resistance at 25C	0.15 Ω
Rated speed	3600 r/min	Inductance ($L_d = L_q$)	2.4 mH
Rated power	47 HP	Total rotational inertia	0.28 Kg·m^2

TABLE III
Control Parameters

SOGI parameter	Value	Positive- and negative-sequence current PI controllers parameter	Value
Gain k	1	Proportional gain	0.5
LPF time const.	20 ms	Integral time const.	30 ms

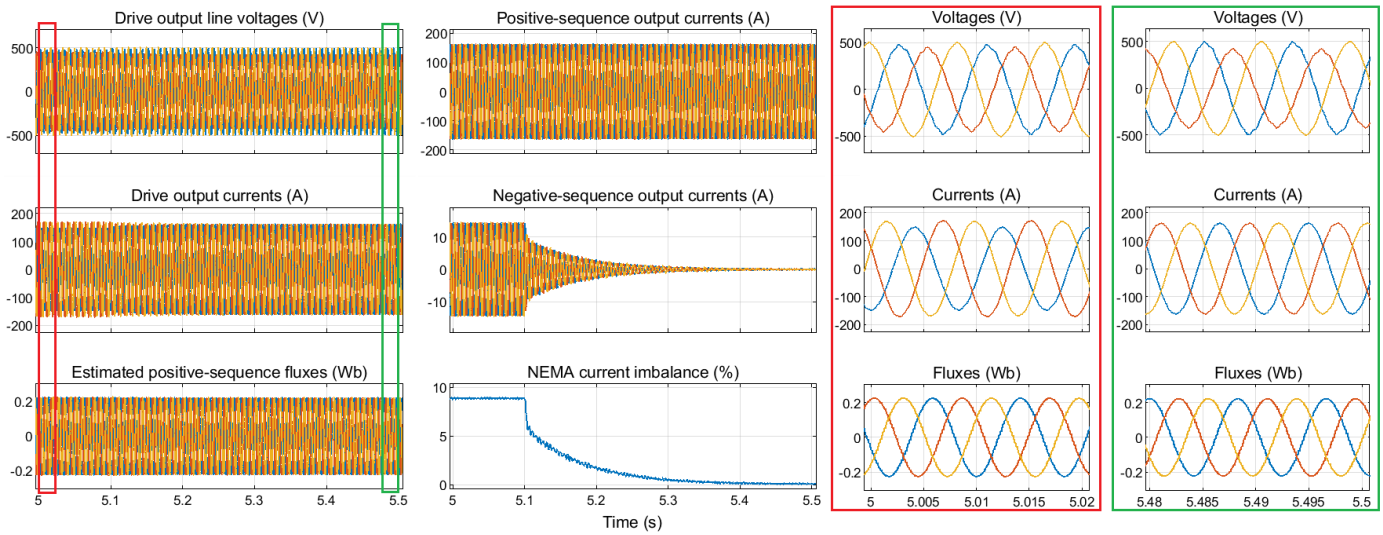

Fig. 10. Simulation results illustrating drive output voltages and currents, estimated positive-sequence fluxes (including magnified extracts on the right), calculated positive- and negative-sequence currents, and percent imbalance, while applying the control method proposed in Fig. 8. Current balancing is enabled at t = 5.1s.

voltages are also imbalanced, as a consequence of unequal voltage drops on the sine filter, as well as of the response of the current controller of Fig. 7a acting on imbalanced currents. At t = 5.1s, current balancing is enabled. The negative-sequence current controller (Fig. 7b) gradually reduces the negative-sequence currents to approximately zero. As a result, the currents at the end of the simulation are balanced, while the drive voltages become more imbalanced due to the addition of the generated negative-sequence voltages. Throughout the simulation, the flux estimator can be seen to generate balanced fluxes, which ensures stable sensorless control.

VI. Experimental Results

The experimental results presented in this section refer to the sensorless control of a PMSM, driven by a 480V-58kVA commercial ESP motor drive through a step-up transformer and long flat armored cable. The drive is also equipped with a sine filter, as shown in Fig. 9. The transformer, cable and motor are shown in Fig. 11, while their main parameters are listed in Tables I and II. The motor drive controller uses the structure of Fig. 8, which was implemented in an Intel Cyclone FPGA. The motor speed is regulated as usual by an outer speed controller loop that provides the current reference $i_{q,ref}$ in Fig. 7a (while $i_{d,ref}$ was set to 0). The values of the SOGI and current controller parameters are listed in Table III.

A. Positive-Sequence Flux Estimation

The first set of results (Figs 12 – 15) focuses on the proposed positive-sequence flux estimation and synchronization method. The purpose is to illustrate the effect of voltage imbalance on the angle estimation based on a conventional integrator and the advantage offered by the application of the proposed method. In the presented results, the motor is running at 1080rpm with a current of approximately 27Arms (50Arms at the drive). Two types of waveform are presented:

- The waveforms shown in Figs. 12 and 14 are obtained using external current probes and a DAC connected to the drive controller board to read the rotor angle estimated by the PLL.
- The waveforms presented in Figs. 13 and 15 are plotted offline, using internal vector control algorithm data (i.e. actual sampled values that are generated and recorded by the digitally implemented system), which runs at a rate of 4kHz.

Figs. 12 and 13 are for the case of using a conventional integrator and HPF to estimate the rotor fluxes for the PLL. It can be clearly seen in Fig. 12 that the measured currents and the estimated rotor angle are heavily distorted. As explained in Section I, the distortion on the estimated angle affects the waveforms of the generated voltages and currents, which in turn further deteriorates the angle estimation. The two oscilloscope shots in Fig. 12 are obtained with a time difference of around 1min, during which the increase of the distortion on all waveforms is evident. Fig. 13 captures the final outcome of this increasing distortion, which is the loss of motor control. In addition to the drive currents and estimated angle, this figure presents the estimated fluxes (middle graph). The fluxes can be seen not to be centered around zero, which hinders angle estimation by the PLL and is responsible for the loss of control.

Figs. 14 and 15 are for the case of using the structure presented in Fig. 6 to estimate the rotor fluxes. The currents and angles in Fig. 14 can be seen to have the expected form (the 5th harmonic appearing on the currents is due to a respective harmonic of the back-EMF of the motor). With reference to Fig. 15, it can be observed that the motor currents (top graph) are imbalanced, which is due to the existence of the flat cable. Although this imbalance can affect the rotor fluxes estimated according to (2), the proposed structure extracts the positive-sequence component of the fluxes and generates a set of balanced signals (middle graph). Based on them, the estimated angle can be seen in the last graph to increase linearly, without any fluctuations, normally caused by imbalanced input signals. As a result, the instability and loss of control appearing under the same test conditions with the conventional integrator is avoided.

(a) (b) (c) (d)

Fig. 11. Photographs of the test setup: (a) VFD, (b) Step-up transformer, (c) Flat armored cable, (d) ESP motor.

B. Current Balancing

The second set of results (Fig. 16) illustrates the effect of enabling the proposed current balancing approach, shown in Fig. 8 for a PMSM. Note that the positive-sequence flux estimation method is enabled at all times in these experiments, thus the estimated angle always follows a clean sawtooth. Fig. 16a presents the three output current waveforms and the estimated angle for the motor running at 3600rpm, before enabling the proposed current balancing algorithm. The RMS values of the three phase currents can be seen on the right and their percent imbalance calculated using the NEMA definition is 8.6%. Fig. 16b illustrates the result of enabling current balancing while running with the same speed and load. The three RMS values can be observed to have become very similar, while their percent imbalance has reduced to 0.5%. The proposed approach was tested using the above setup over a wide range of motor speeds, from approximately 100 to 4000rpm and loads (without a step-up transformer for speeds below 500rpm). For the entire range, the measured percent imbalance was in the order of 9%, and was suppressed to below 1% by enabling the proposed algorithm. Part of the remaining imbalance is thought to be due to tolerances and calibration errors of the drive current sensors and resolution of the algorithm arithmetic. The method was also tested successfully with higher-power drives, rated up to 260kVA.

VII. Discussion

This section discusses a number of points relating to the application of the proposed method at low or negative motor speeds.

Motor control at low (as compared to rated) speeds is known to present challenges due to the operation of the motor drives with low output voltage and electrical frequency. For drives that do not employ output voltage sensors, thus rely on the reference (demanded) voltages to derive the output voltages, the accuracy of flux estimation can be limited when operating in the low-voltage range. This is because the effect of various inverter nonlinearities, occurring mainly due to dead time and voltage drop across semiconductors, become more evident in this range [37]. The drives used in the performed experiments are equipped with output voltage sensors, but the proposed method did not need to make use of the measured voltages for speeds above 500rpm, which corresponds to approximately 14% of the motor rated speed. The use of reference voltages (including a compensation for the sine filter voltage drop) did not adversely affect flux estimation and current balancing in these speeds, which cover the entire range of ESP operation. Measured voltages were used for experiments at very low speeds and enabled operation down to 100rpm, without the use of a step-up transformer, as mentioned in Section VI-*B*. In drives without output voltage sensors, the proposed method could use, instead of the reference voltages, estimates of the output voltages obtained by means of techniques such as the volt-second sensing presented in [38].

Another aspect relating to low-speed operation is motor starting. Particularly with reference to PMSMs, starting typically involves an open-loop (i.e. not using the observer) speed ramp based on a constant V/f or I-f strategy, and a method for smoothly transitioning to sensorless operation above a certain speed [3], [5], [8], [39]. The VFDs used for the experiments follow a starting approach of the I-f type, which did not have to be modified to encompass the proposed method. The method was initiated during the speed ramp, simply with the difference of using the open-loop reference angular frequency in the place of the observer-estimated ω_{est} in Fig. 6.

Finally, a point to be mentioned relates to the operation of the proposed method with negative motor speeds. The angular frequency required by the SOGIs should never be negative, thus for negative speeds it must be made equal to the absolute value of ω_{est}. Moreover, since the sequence between the voltages and currents of the three phases is different when a motor runs in reverse, it is the positive-sequence quantities that represent the imbalance in this case. Thus, the positive- and negative-sequence flux and current estimates must be alternated in all their occurrences for the method to function. This is straightforward if the motor is stopped, but needs to be addressed in applications that require the speed to be reversed while the motor is running (on the fly).

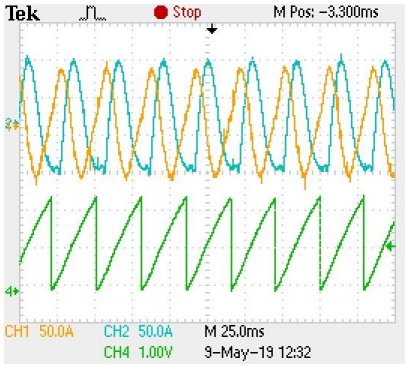

(a)

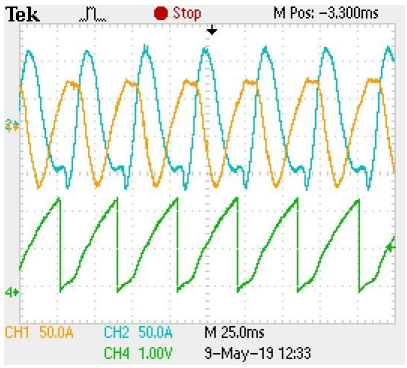

(b)

Fig. 12. Oscilloscope shots illustrating two drive currents and the estimated rotor angle while using a conventional integrator. The results in (a) and (b) were obtained with a time difference of approximately 1min to illustrate the increasing distortion.

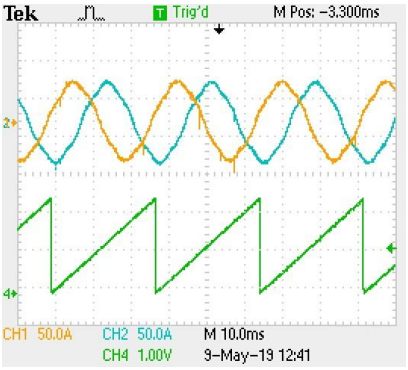

(a)

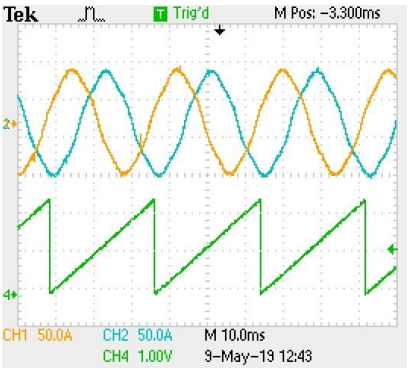

(b)

Fig. 14. Oscilloscope shots illustrating two drive currents and the estimated rotor angle while using the proposed structure, for two different motor loads.

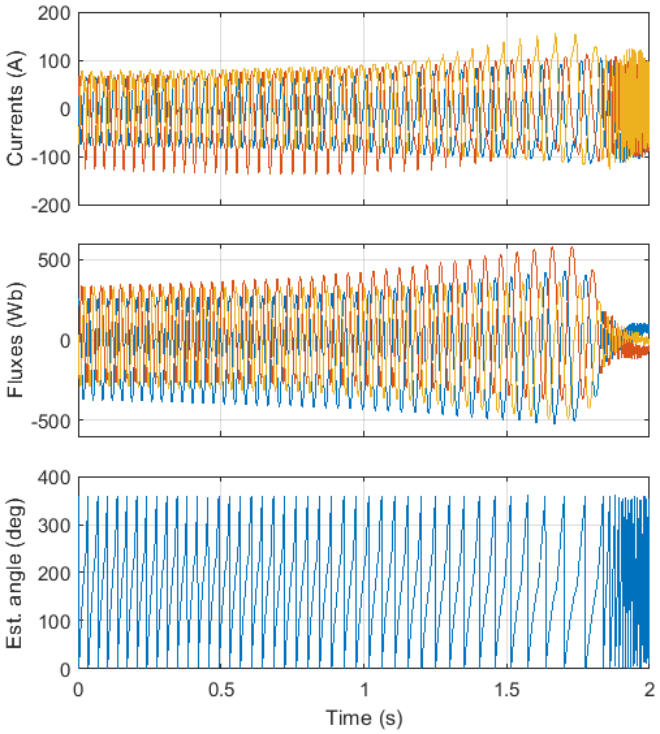

Fig. 13. Internal vector control algorithm data for the last 2s before loss of control while using a conventional integrator.

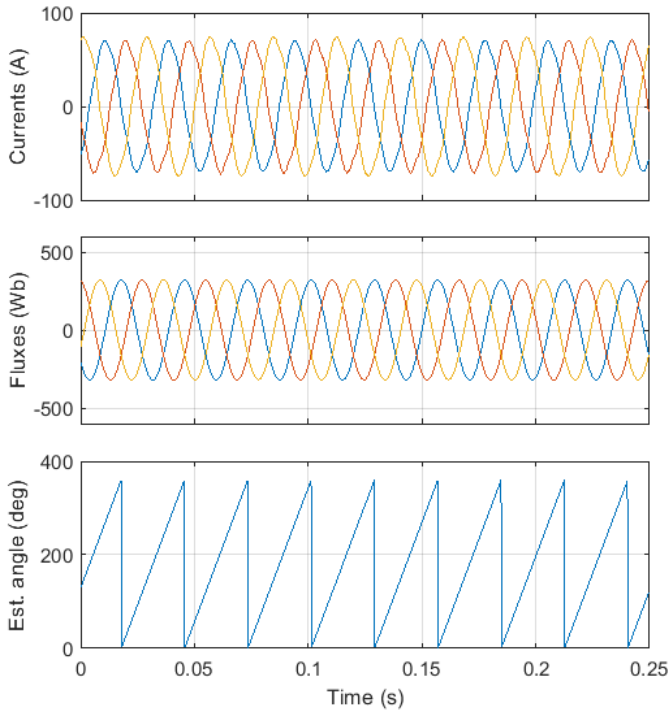

Fig. 15. Internal vector control algorithm data while using the proposed structure, illustrating stable operation.

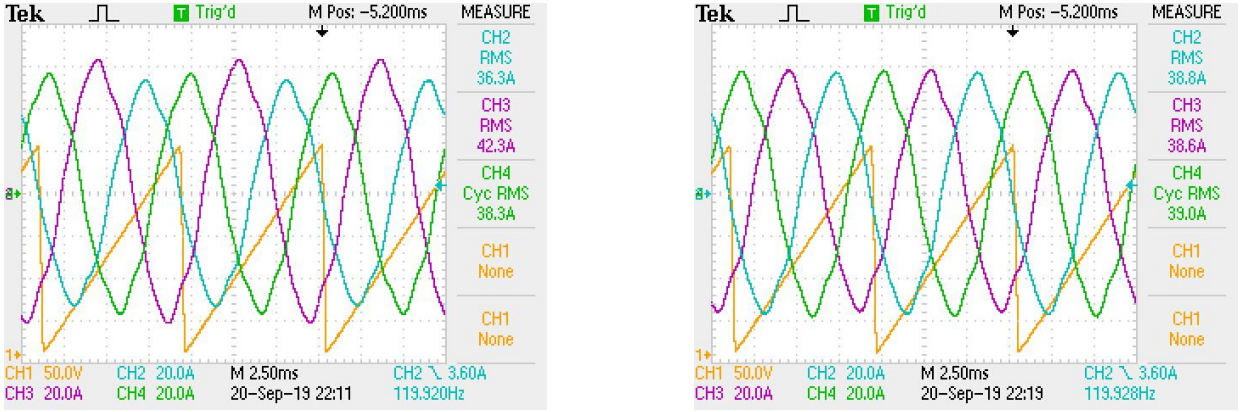

Fig. 16. Three-phase currents, estimated rotor angle and RMS current values at 3600 rpm (a) without, (b) with current balancing.

VIII. Conclusion

This paper presented a comprehensive approach to solving the problem of sensorless control and current balancing for motor drives operating under imbalanced conditions. It relied on the use of SOGI, the state-of-the-art structure for frequency-adaptive filtering, integration and quadrature signal generation, to produce a positive-sequence flux estimator and a negative-sequence current estimator. The two estimators were combined in a computationally efficient manner to form single structure for sensorless motor control, capable of providing both stable control and current balancing. The effectiveness of the proposed approach was demonstrated through extensive experimental results using actual oil-field (ESP) system components.

References

[1] T. R. Brinner, "Voltage and Cable Impedance Unbalance in Submergible Oil Well Pumps," in *IEEE Transactions on Industry Applications*, vol. IA-20, no. 1, pp. 97-104, Jan. 1984.

[2] M. Bendjedia, A. Khlaief and M. Boussak, "Sensorless speed control of outrunner PMSM drive connected to long cable for flying remote operative vehicle," *2012 International Conference on Electrical Machines*, Marseille, France, 2012, pp. 2252-2258.

[3] D. Stellas, M. T. Hansen, T. Thiringer, T. Strømsvik and H. B. Ulvestad, "Position-sensorless control of a submersible PMSM fed over a long cable and two transformers," *2014 16th European Conference on Power Electronics and Applications*, Lappeenranta, Finland, 2014, pp. 1-10.

[4] R. Picatoste, M. Butcher and A. Masi, "Current control strategy for electric motor drives using long cables," *2017 IEEE 26th International Symposium on Industrial Electronics (ISIE)*, Edinburgh, UK, 2017, pp. 257-262.

[5] S. F. Rabbi, M. Constantine and M. A. Rahman, "A novel sensorless IPM motor drive for electric submersible pumps," *2017 IEEE International Electric Machines and Drives Conference (IEMDC)*, Miami, FL, USA, 2017, pp. 1-8.

[6] G. da Cunha, A. J. Rossa, J. A. Alves and E. Cardoso, "Control of Permanent Magnet Synchronous Machines for Subsea Applications," in *IEEE Transactions on Industry Applications*, vol. 54, no. 2, pp. 1899-1905, March-April 2018.

[7] X. Liang and A. El-Kadri, "Factors Affecting Electrical Submersible Pump Systems Operation," *2018 IEEE Electrical Power and Energy Conference (EPEC)*, Toronto, ON, Canada, 2018, pp. 1-6.

[8] Z. Li et al., "Sensorless Starting Control of Permanent Magnet Synchronous Motors with Step-up Transformer for Downhole Electric Drilling," *IECON 2018 - 44th Annual Conference of the IEEE Industrial Electronics Society*, Washington, DC, USA, 2018, pp. 689-694.

[9] L. Ding, Y. W. Li, N. R. Zargari and R. Paes, "Sensorless Control of CSC-Fed PMSM Drives with Low Switching Frequency for Electrical Submersible Pump Application," in *IEEE Transactions on Industry Applications*, vol. 56, no. 4, pp. 3799-3808, July-Aug. 2020.

[10] Š. Janouš, J. Talla, T. Košan and Z. Peroutka, "Predictive control of induction motor drive with transformer," *2020 19th International Conference on Mechatronics - Mechatronika (ME)*, Prague, Czech Republic, 2020, pp. 1-6.

[11] P. Xie, D. Dewar, G. Vakil and C. Gerada, "Gain-scheduled LQR control of an aerospace drive system with LC filter and long feeder cable," *2020 23rd International Conference on Electrical Machines and Systems (ICEMS)*, Hamamatsu, Japan, 2020, pp. 656-661.

[12] J. Timmerberg and S. Mylvaganam, "Inductance of 3-phase transmission lines of different layouts with focus on cables in flat formation," *2016 12th IEEE International Symposium on Electronics and Telecommunications (ISETC)*, Timisoara, Romania, 2016, pp. 235-238.

[13] P. Rodriguez, J. Pou, J. Bergas, I. Candela, R. Burgos and D. Boroyevic, "Double Synchronous Reference Frame PLL for Power Converters Control," *2005 IEEE 36th Power Electronics Specialists Conference*, Recife, 2005, pp. 1415-1421.

[14] M. Reyes, P. Rodriguez, S. Vazquez, A. Luna, R. Teodorescu and J. M. Carrasco, "Enhanced Decoupled Double Synchronous Reference Frame Current Controller for Unbalanced Grid-Voltage Conditions," in *IEEE Transactions on Power Electronics*, vol. 27, no. 9, pp. 3934-3943, Sept. 2012.

[15] D. Yazdani, M. Mojiri, A. Bakhshai and G. JoÓs, "A Fast and Accurate Synchronization Technique for Extraction of Symmetrical Components," in *IEEE Transactions on Power Electronics*, vol. 24, no. 3, pp. 674-684, March 2009.

[16] S. B. Singh, A. K. Singh and P. Thakur, "Accurate performance assessment of IM with approximate current unbalance factor for NEMA definition," *2014 16th International Conference on Harmonics and Quality of Power (ICHQP)*, Bucharest, Romania, 2014, pp. 674-678.

[17] M. Tsypkin, "The origin of the electromagnetic vibration of induction motors operating in modern industry: Practical experience — Analysis and diagnostics," *2016 Petroleum and Chemical Industry Technical Conference (PCIC)*, Philadelphia, PA, USA, 2016, pp. 1-9.

[18] S. Sahu, R. N. Dash, C. K. Panigrahi and B. Subudhi, "Unbalanced voltage effects and its analysis on an induction motor," *2017 International Conference on Innovative Mechanisms for Industry Applications (ICIMIA)*, Bengaluru, India, 2017, pp. 263-268.

[19] J. M. Tabora, M. E. De Lima Tostes, E. O. De Matos, U. H. Bezerra, T. M. Soares and B. S. De Albuquerque, "Assessing Voltage Unbalance Conditions in IE2, IE3 and IE4 Classes Induction Motors," in *IEEE Access*, vol. 8, pp. 186725-186739, 2020.

[20] M. Ciobotaru, R. Teodorescu, F. Blaabjerg. A new single phase PLL structure based on second order generalized integrator. *IEEE Power Electronics Specialists Conference*, pp. 1-6, 2006.

[21] J. Li, J. Zhao, J. Wu and P. p. Xu, "Improved dual second-order generalized integrator PLL for grid synchronization under non-ideal

grid voltages including DC offset," *2014 IEEE Energy Conversion Congress and Exposition (ECCE)*, Pittsburgh, PA, 2014, pp. 136-141.
[22] W. Xu, Y. Jiang, C. Mu and F. Blaabjerg, "Improved Nonlinear Flux Observer-Based Second-Order SOIFO for PMSM Sensorless Control," in *IEEE Transactions on Power Electronics*, vol. 34, no. 1, pp. 565-579, Jan. 2019.
[23] P. Rodríguez, R. Teodorescu, I. Candela, A. V. Timbus, M. Liserre and F. Blaabjerg, "New positive-sequence voltage detector for grid synchronization of power converters under faulty grid conditions," *2006 37th IEEE Power Electronics Specialists Conference*, Jeju, 2006, pp. 1-7.
[24] K. Możdżyński, "Simple digital integration algorithm with saturation and drift elimination based Second-Order Generalized Integrator," *2015 9th International Conference on Compatibility and Power Electronics (CPE)*, Costa da Caparica, 2015, pp. 312-316.
[25] G. Wang *et al*., "Enhanced Position Observer Using Second-Order Generalized Integrator for Sensorless Interior Permanent Magnet Synchronous Motor Drives," in *IEEE Transactions on Energy Conversion*, vol. 29, no. 2, pp. 486-495, June 2014.
[26] Y. Jiang, W. Xu and C. Mu, "Improved SOIFO-based rotor flux observer for PMSM sensorless control," *IECON 2017 - 43rd Annual Conference of the IEEE Industrial Electronics Society*, Beijing, 2017, pp. 8219-8224.
[27] B. Liu, B. Zhou and T. Ni, "Principle and Stability Analysis of an Improved Self-Sensing Control Strategy for Surface-Mounted PMSM Drives Using Second-Order Generalized Integrators," in *IEEE Transactions on Energy Conversion*, vol. 33, no. 1, pp. 126-136, March 2018.
[28] I. Ralev, A. Klein-Hessling, B. Pariti and R. W. De Doncker, "Adopting a SOGI filter for flux-linkage based rotor position sensing of switched reluctance machines," *IEEE International Electric Machines and Drives Conference (IEMDC)*, Miami, FL, 2017, pp. 1-7.
[29] R. Zhao, Z. Xin, P. C. Loh and F. Blaabjerg, "A novel flux estimator based on SOGI with FLL for induction machine drives," *2016 IEEE Applied Power Electronics Conference and Exposition (APEC)*, Long Beach, CA, 2016, pp. 1995-2002.
[30] Z. Xin, R. Zhao, F. Blaabjerg, L. Zhang and P. C. Loh, "An Improved Flux Observer for Field-Oriented Control of Induction Motors Based on Dual Second-Order Generalized Integrator Frequency-Locked Loop," in *IEEE Journal of Emerging and Selected Topics in Power Electronics*, vol. 5, no. 1, pp. 513-525, March 2017.
[31] R. Zhao, Z. Xin, P. C. Loh and F. Blaabjerg, "A Novel Flux Estimator Based on Multiple Second-Order Generalized Integrators and Frequency-Locked Loop for Induction Motor Drives," in *IEEE Transactions on Power Electronics*, vol. 32, no. 8, pp. 6286-6296, Aug. 2017.
[32] P. Rodriguez, A. Luna, M. Ciobotaru, R. Teodorescu and F. Blaabjerg, "Advanced Grid Synchronization System for Power Converters under Unbalanced and Distorted Operating Conditions," *IECON 2006 - 32nd Annual Conference on IEEE Industrial Electronics*, Paris, 2006, pp. 5173-5178.
[33] P. Rodriguez, A. Luna, I. Candela, R. Mujal, R. Teodorescu and F. Blaabjerg, "Multiresonant Frequency-Locked Loop for Grid Synchronization of Power Converters Under Distorted Grid Conditions," in *IEEE Transactions on Industrial Electronics*, vol. 58, no. 1, pp. 127-138, Jan. 2011.
[34] G. Orfanoudakis and M. Yuratich, "SOGI-based integrator, PLL and current controller for grid connection and motor control," International patent publication number WO 2018/157120 A1, 2018.
[35] G. I. Orfanoudakis, S. M. Sharkh and M. A. Yuratich, "Positive-sequence flux estimator based on Second-Order Generalized Integrators for grid synchronization and motor control under imbalanced conditions," *2019 21st European Conference on Power Electronics and Applications (EPE '19 ECCE Europe)*, Genova, Italy, 2019, pp. 1-10.
[36] "Definitions of Voltage Unbalance," in IEEE Power Engineering Review, vol. 21, no. 5, pp. 49-51, May 2001.
[37] R. W. Hejny and R. D. Lorenz, "Evaluating the Practical Low-Speed Limits for Back-EMF Tracking-Based Sensorless Speed Control Using Drive Stiffness as a Key Metric," in *IEEE Transactions on Industry Applications*, vol. 47, no. 3, pp. 1337-1343, May-June 2011.
[38] Y. Wang, Y. Xu, N. Niimura, B. D. Rudolph and R. D. Lorenz, "Using Volt-Second Sensing to Directly Improve Torque Accuracy and Self-Sensing at Low Speeds," in *IEEE Transactions on Industry Applications*, vol. 53, no. 5, pp. 4472-4482, Sept.-Oct. 2017.
[39] M. Fatu, R. Teodorescu, I. Boldea, G. Andreescu and F. Blaabjerg, "IF starting method with smooth transition to EMF based motion sensorless vector control of PM synchronous motor/generator," *IEEE Power Electronics Specialists Conference*, Rhodes, Greece, 2008, pp. 1481-1487.

Georgios I. Orfanoudakis (M'14) received his MEng in electrical engineering and computer science from the National Technical University of Athens (NTUA), Greece, in 2007, and his PhD on power electronic converters from the University of Southampton, UK, in 2013.

From 2012 until 2019 he worked with the University of Southampton as a Research Associate (2012-2014), the Hellenic Mediterranean University as a Teaching Fellow (2014-2019) and with TSL Technology Ltd, as a Power Electronics R&D Engineer. In 2020 he was appointed by the Electrical and Computer Engineering department of the Hellenic Mediterranean University, Crete, Greece, as an Assistant Professor of Power Electronics and Motor Drives. His research focuses on topologies and modulation strategies of multilevel and PV inverters, and on sensorless control of motor drives.

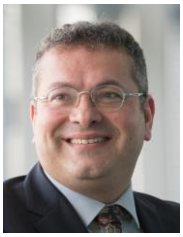

Suleiman M. Sharkh is Professor of Power Electronics, Machines and Drives in the Faculty of Engineering and the Physical Sciences at the University of Southampton. He the Deputy Director of the Southampton EPSRC Energy Storage and its Applications Centre for Doctoral Training and was past Head of the Mechatronics Research Group.

He has over 20 years research experience in electric machines, power electronics and their applications in transport, renewable energy and microgrids. He has published over 160 papers, supervised over 20 PhD students to completion. His inventions and research, funded by industry, EPSRC and Innovate UK, have contributed to the development of several commercial products: rim driven thrusters; direct drive tidal turbine generators; submersible motors; high speed PM machines for electric turbo compounding and gas compressors; grid connected inverters; novel electric motors with integrated clutch for hybrid marine vessel propulsion; and multi-axis actuators with adjustable resonance frequency for active vibration damping.

Prof Sharkh was the winner of The Engineer Energy Innovation and Technology Award 2008 for his work on novel rim driven marine thrusters and turbine generators. He is a Senior Member of the IEEE, a member of the IET and a Chartered Engineer.

Michael A Yuratich is Managing Director of TSL Technology Limited and co-founder of Magnetic Pumping Solutions LLC. He received his BSc(Hons) in Electronics Science in 1974 and his PhD in Nonlinear Optics in 1977, subsequently becoming Ramsay Memorial Fellow and lecturer

in Electronics, all at the University of Southampton. At the University of Southampton, he also contributed to the Industrial Mathematics MSc course and is a Visiting Scholar.

In his industrial career he has worked widely in electro-mechanical systems and instrumentation for downhole exploration equipment. He has worked intensively for over twenty years on development and commercialization of specialist permanent magnet machines up to 1500kW: motors, generators and integrated subsea thrusters, with associated development and commercialization of variable speed drives and vector control algorithms. He holds 65 patents and has published 20 papers and a book.

Dr Yuratich was the winner of The Engineer Energy Innovation and Technology Award 2008 for integrated thrusters, and twice winner of Society of Petroleum Engineer technology awards. He is a Chartered Physicist.